PHYSICS AND CHEMISTRY OF SOLID STATE
V. 26, No. 2 (2025) pp. 420-425
Section: Physics

DOI: 10.15330/pcss.26.2.420-425

Vasyl Stefanyk Precarpathian National University

ФІЗИКА І ХІМІЯ ТВЕРДОГО ТІЛА
Т. 26, № 2 (2025) С. 420-425
Фізико-математичні науки

PACS: 71.15.Mb; 71.20. ± b; 71.20.Nr.

ISSN 1729-4428 (Print)
ISSN 2309-8589 (Online)

S.V. Syrotyuk[1], M.K. Hussain[2], R.A. Nakonechnyi[1]

Electronic and magnetic properties of hexagonal ZnSeS solid solutions modified by Cr impurity and the anion concentration

[1]*Lviv Polytechnic National University, Lviv, Ukraine, stepan.v.syrotiuk@lpnu.ua;*
[2]*Department of Electrical Power Techniques Engineering, AL-Hussain University College, Kerbala, Iraq*

The spin-polarized electronic energy spectra of the ZnSeS solid solution were obtained based on calculations for the supercell containing 64 atoms. The electronic properties of the materials based on the two supercells, namely $Zn_{31}Cr_1Se_8S_{24}$ and $Zn_{31}Cr_1Se_{24}S_8$, were calculated, where Cr replaces the Zn atom. The calculation results reveal that the both materials are semiconductors for the spin down electronic states. For the opposite spin momentum of electrons both materials show the matallic states. For both materials, a significant effect of the substitutional Cr impurity on their electronic and magnetic properties has been established. Both materials investigated here are semimetals, so they are promising materials for spin electronics.

Keywords: ZnSeS Solid Solutions, 3d Impurity, Electronic Energy Bands, Magnetic Moment.

Received 31 January 2025; Accepted 14 July 2025.

Introduction

ZnS and ZnSe present identical crystal structures, the cubic zinc blende ($F43m$) and the hexagonal wurtzite-2H ($P63mc$), with small lattice parameter mismatches and they can form a complete ZnS_xSe_{1-x} solid solution [1]. The band-gap energy, Eg, of this solid solution changes continuously with the composition according to a quadratic function,

$$E_g(x) = xE_g^{ZnS} + (1-x)E_g^{ZnSe} - bx(1-x),$$

with a bowing parameter, b, in the 0.35–0.68 eV range [2–4].

Therefore, if this solid solution is properly doped with Mn2+, by controlling its stoichiometry, it would be possible to tune the band edge excitation of the host material from ultraviolet to blue region, but keeping the emission wavelength constant at ~585 nm [1].

High-quality ternary ZnS_xSe_{1-x} nanowires (NWs) with tunable band-gaps were synthesized by a chemical vapor deposition (CVD) method. Photoluminescence (PL), absorption and Raman spectra were carried out to study their optical properties, revealing that the band-gaps of NWs can be accurately controlled and cover the entire range from 2.65 eV to 3.7 eV by changing the component ratio. Optoelectronic properties were further studied by constructing photodetectors (PDs), which exhibited a high responsivity of $1.5\times10^6 AW^{-1}$, a photoconductive gain of 4.5×10^6 and fast response speed of 520/930 μs. Such high performances are superior to the previous reported results, indicating these ternary ZnS_xSe_{1-x} nanostructures will have great potential applications in nano-optoelectronic devices [5].

II-VI materials are intensively studied now within the framework of various theoretical approaches. In particular, the kinetic properties of the CdTe material were recently studied from the first principles in the formalism of projection augmented waves (PAW, projector augmented waves) [6]. The electronic, phonon, optical, and thermodynamic properties of the CdTe crystal were studied on the basis of the density functional theory (DFT) using the pseudopotential method [7]. The same theoretical approach was successfully applied to study the electronic structure of CdSeTe solid solutions [8].

The existence of localized energy levels in the band gaps of group IV, III-V, and II-VI semiconductors doped with transition-metal TM impurities leads to rich optical

and magnetic phenomenologies [9]. In the recent two decades, transition metal (TM) doped II-VI compounds, especially Cr^{2+}:ZnSe materials, have proven to be the most promising candidates for room-temperature tunable Mid-IR lasers [10, 11]. For the Cr^{2+}:ZnSe laser materials, the divalent chromium ion incorporated into the ZnSe lattice occupies the zinc site, which is coordinated by four selenium anions. Because of the presence of the heavier anions Se, which decreases the phonon cut-off frequency, there is almost no temperature quenching in the Mid-IR band and the quantum efficiency is close to 100% at room temperature.

ZnX chalcogenides (X=S, Se, Te) were devoted to a number of experimental and theoretical studies of their electronic and optical properties [12, 13].

However, studies of II-VI solid solutions with impurities of transition elements are currently rare [14–16].

The purpose of this work is to study the influence of anion concentrations on the electronic and magnetic properties of the Cr:ZnSeS crystal. Calculations were performed in a 2 × 2 × 2 supercell containing 64 atoms.

I. Theory and calculation details

To calculate the optical constants and kinetic coefficients of crystals, it is necessary to have a true wave function $\psi_\alpha(r)$. The projector augmented waves (PAW) [17, 18] combine the features of the pseudopotential and the all-electronic approach of augmented plane waves. The wave $\psi_\alpha(r)$ and pseudo-wave $\tilde{\psi}_\alpha(r)$ functions are related to each other as follows:

$$|\psi_n(r)>=\tau|\tilde{\psi}_n(r)>, \quad (1)$$

where the operator

$$\tau = 1 + \sum_\alpha \sum_i \left(|\phi_i^\alpha> - |\tilde{\phi}_i^\alpha>\right) < \tilde{p}_i^\alpha| \quad (2)$$

is defined by the atomic wave function $|\phi_i^\alpha(\mathrm{r})>$, atomic pseudo-wave function $|\tilde{\phi}_i^\alpha(\mathrm{r})>$ and the projector function $<\tilde{p}_i^\alpha|$.

The summation in (2) is carried out over the augmentation spheres, which are numbered with the index a, and the index $i = \{n, l, m\}$ corresponds to the principal, orbital, and magnetic quantum numbers, respectively.

The stationary Schrödinger equation

$$H|\psi_n>=|\psi_n>\varepsilon_n, \quad (3)$$

taking into account (2), takes the following form:

$$\tau^+ H\tau|\tilde{\psi}_n>=\tau^+\tau|\tilde{\psi}_n>\varepsilon_n, \quad (4)$$

where the desired electron spectrum is the same as in equation (3).

The idea of the PAW method is to transform the Schrödinger equation into an equation in which the unknown state function is $|\tilde{\psi}_n>$. If it is known, then by means of (1) the true electronic function of the state $|\tilde{\psi}_n>$ is obtained. Using the latter, we find the electron density and the corresponding Hartree potential

The exchange-correlation potential was chosen in the PBE0 form [19, 20], according to which the exchange-correlation energy functional

$$E_{xc}^{PBE0}[\rho] = E_{xc}^{PBE}[\rho] + \frac{1}{4}(E_x^{HF}[\psi_{3d}] - E_x^{PBE}[\rho_{3d}]), \quad (5)$$

where PBE corresponds to the exchange-correlation functional [19], and ψ_{3d}, ρ_{3d} denote the wave function and electron density the Cr atom.

Tables 1 and 2 show the reduced atomic coordinates of the unoptimized and optimized structures.

Table 1.

Initial and optimized reduced atomic coordinates for a smaller supercell of a $Zn_4Se_3S_1$ solid solution

Coords	Initial			Optimized		
Atom	x/a	y/b	z/c	x/a	y/b	z/c
S	0	0	0.1874	0	0	0.1927
S	0.3333	0.6666	0.4375	0.3333	0.6666	0.4379
S	0	0	0.6874	0	0	0.6823
Se	0.6666	0.3333	0.9375	0.6666	0.3333	0.9363
Zn	0	0	0	0	0	0.0088
Zn	0.3333	0.6666	0.2500	0.3333	0.6666	0.2527
Zn	0	0	0.5	0	0	0.4975
Zn	0.6666	0.3333	0.75	0.6666	0.3333	0.7418

Table 2.

Initial and optimized reduced atomic coordinates for a smaller supercell of a $Zn_4Se_1S_3$ solid solution

Coords	Initial			Optimized		
Atom	x/a	y/b	z/c	x/a	y/b	z/c
S	0	0	0.1877	0	0	0.1879
S	0.3333	0.6666	0.4321	0.3333	0.6667	0.4323
S	0	0	0.6865	0	0	0.6867
Se	0.6666	0.3333	0.9421	0.6666	0.3333	0.9419
Zn	0	0	0.0081	0	0	0.0082
Zn	0.3333	0.6666	0.2426	0.3333	0.6667	0.2423
Zn	0	0	0.4980	0	0	0.4980
Zn	0.6666	0.3333	0.7528	0.6666	0.3333	0.7527

The starting lattice lenghts were equal to (7.53403, 7.53403, 24.78802), and the optimized parameters were (7.55834, 7.55834, 24.82234) a.u., respectively. The initial and final pressure values were equal to 0.75 and 0.013 GPa. The initial and final lattice angles were equal to (90.0, 90.0, 120.0) degrees, corresponding to the wurtzite structure.

The starting lattice lenghts were equal to (7.53403, 7.53403, 24.78802), and the optimized parameters were (7.37003, 7.37003, 24.15705) a.u., respectively. The initial and final pressure values were equal to 1.0 and 0.00001 GPa, respectively. The initial and final lattice angles were equal to (90.0, 90.0, 120.0) degrees, corresponding to the wurtzite structure.

Two variants of calculations were performed in 2×2×2 supercells using the Abinit program [17] in the PAW basis.

1. The Cr:ZnSeS supercell contains 64 atoms, and its formula unit is $Zn_{31}Cr_1Se_8S_{24}$, that is, one Zn atom is replaced by an Cr atom.

2. The Cr:ZnSeS supercell contains 64 atoms, and its formula unit is $Zn_{31}Cr_1Se_{24}S_8$, that is, one Zn atom is replaced by an Cr atom.

Both materials considered here are described by the space group Cm (No. 8) and the Bravais lattice mC (face-center monoclinic). Whereas the pure wurtzite crystal ZnS is characterized by the space group symmetry $P6_3mc$ (No. 186) and the Bravais lattice hP (primitive hexagonal).

Structural optimization was performed in two stages. The first stage consisted of optimizing the crystal lattice parameters. The second stage optimized the values of the atomic coordinates in the cell. A spatial grid of 30×30×100 was used to calculate the wave function, and the fine 60×60×200 grid was applied for evaluation of the electron density and crystal potential.

II. Results and discussions

Figure 1 shows the spin-polarized electronic energy spectra of the Cr:ZnSeS crystals. These results were obtained for materials with different anion concentrations, i.e. $Zn_{31}Cr_1Se_8S_{24}$ and $Zn_{31}Cr_1Se_{24}S_8$. A comparison of dispersion laws reveals that for spin up electronic states both materials show metallic properties. Indeed, the Fermi level for these states intersects the dispersion curves that correspond most closely to the d states of the Cr atom. For electrons with opposite spin orientations, both materials exhibit semiconductor properties. In the material with a higher S content, the Fermi level is localized in the middle of the band gap, i.e., as in a classical semiconductor. But in the material with a higher Se content, the Fermi level is shifted toward the conduction band. The band gaps for both materials, corresponding to electrons with spin down, equal to 1.88 and 1.64 eV, recpectively.

Figure 2 shows the spin-polarized densities of electronic states of Zn for both materials. From Figure 2, it can be seen that the partial densities of electronic states in the conduction band exhibit a weak dependence on the composition of the anionic subsystem. However, in the valence band, which reflects the electron-populated states, there is a noticeable redistribution of the partial densities of states.

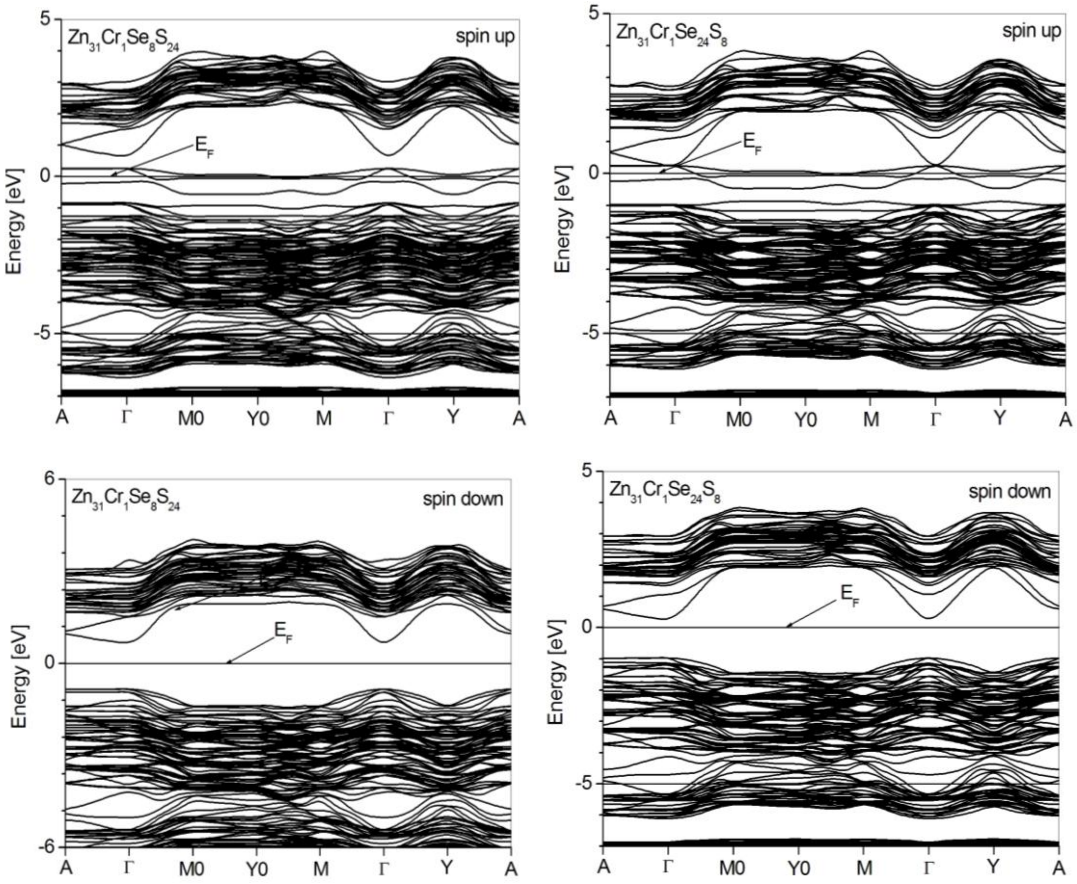

Fig. 1. Spin-polarized electronic energy spectra of the Cr:ZnSeS materials.

Figure 3 shows the spin-polarized densities of electronic states of the Cr atom for both materials. The curves depicted on it reveal a significant sensitivity of the partial DOS of the Cr atom to the concentration of anions in the supercell. The partial DOS of the 3d electrons of the Cr atom are particularly sensitive to the anionic composition of the supercell. The partial densities of 3d states of Cr corresponding to supercells $Zn_{31}Cr_1Se_8S_{24}$ and $Zn_{31}Cr_1Se_{24}S_8$ show significant differences in the valence band, in the vicinity of the Fermi level, and also in the conduction band.

In Fig. 4 are shown the spin-polarized partial densities of electronic states of Se in the Cr:ZnSeS material, calculated under normal conditions. The curves of the density of states for the material with defects (vac) reveal the presence of the Se p states at the Fermi level for both values of the spin moment.

Figure 5 shows the spin-polarized total DOS for the Cr:ZnSeS materials. The curves of the total DOS of both materials, containing various amounts of Se and S, exhibit semimetallic properties. That is, for spin up they are metals, and for spin down they have semiconductor properties.

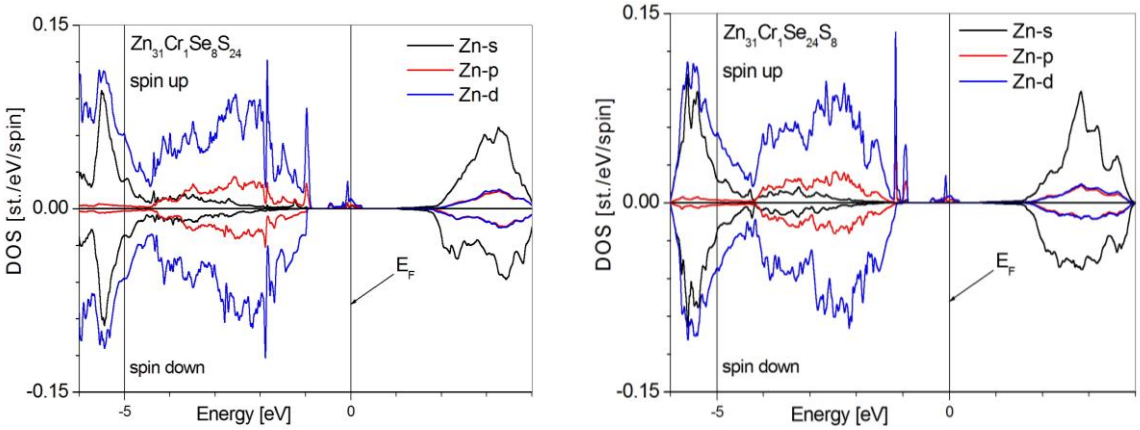

Fig. 2. The Zn partial density of electronic states in the Cr:ZnSeS materials.

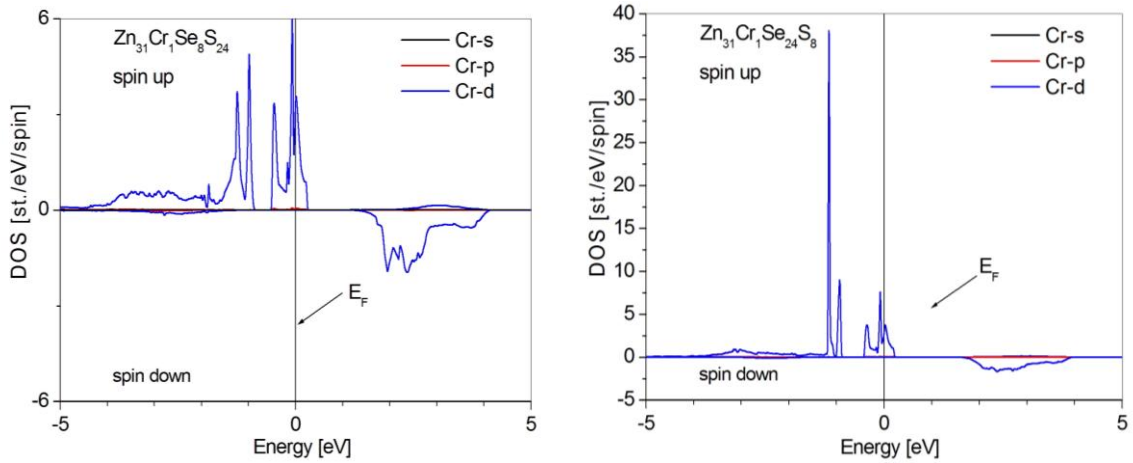

Fig. 3. The Cr partial density of electronic states in the Cr:ZnSeS materials.

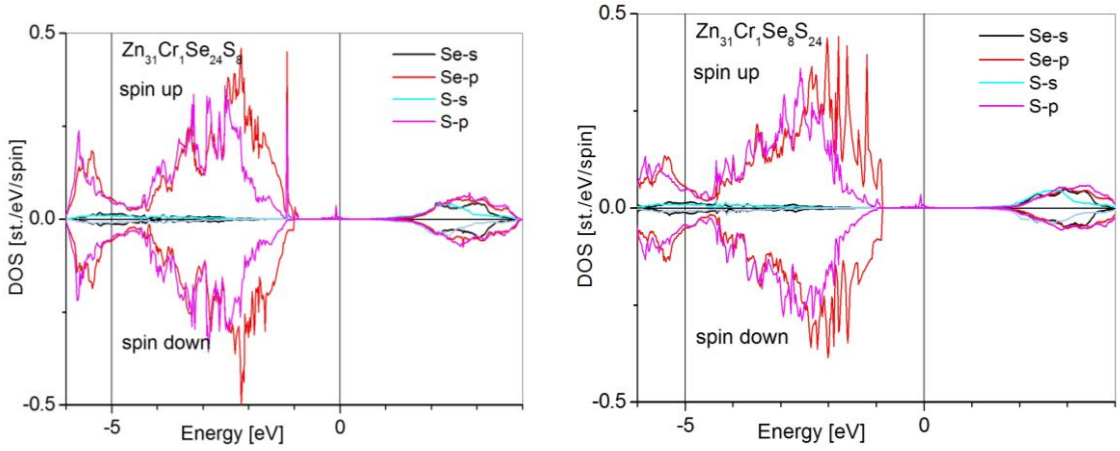

Fig. 4. The partial electronic DOS on the Se and S atoms in the Cr:ZnSeS materials.

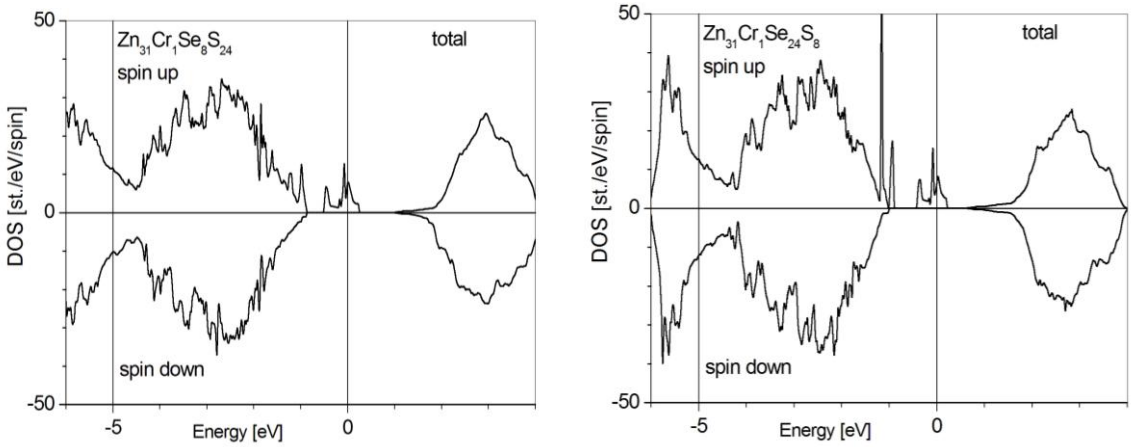

Fig. 5. The Zn partial density of electronic states in the Cr:ZnSeS material.

The magnetic moment of the supercell $Zn_{31}Cr_1Se_8S_{24}$ is 4 μ_B, and the contribution of the Cr atom is 3 μ_B,. For the supercell $Zn_{31}Cr_1Se_{24}S_8$, these values are 4 μ_B, and 3.05 μ_B,, respectively.

Conclusion

The spin-polarized electronic energy spectra of the Cr:ZnSeS system were obtained for the 2 × 2 × 2 supercell. The electronic structure of the Cr:ZnSeS material, represented by supercells $Zn_{31}Cr_1Se_8S_{24}$ and $Zn_{31}Cr_1Se_{24}S_8$, reveal semiconducting properties for spin down spin orientations. For the opposite spin moments both materials show metallic properties. It is especially worth emphasizing the significant differences in the partial DOS of the 3d electrons on the Cr atom. These differences are clearly evident in the valence band, in the vicinity of the Fermi level, and also in the conduction band.

Acknowledgements

This contribution was created under the support of the High Performance Computing Laboratory at the Lviv Polytechnic National University.

Syrotyuk S.V. – PhD, Prof. Assoc., Lviv Polytechnic National University;
Hussain M.K. – PhD, Prof. Assoc., AL-Hussain University College, 56001 Kerbala, Iraq;
Nakonechnyi R.A. – Dr. Engineering Sci., PhD., Prof. Assoc., Lviv Polytechnic National University.

[1] M.A. Avil´es, F.J. Gotor, *Tuning the excitation wavelength of luminescent Mn2+-doped ZnSxSe1-x obtained by mechanically induced self-sustaining reaction*, Optical Materials 117, 111121 (2021); https://doi.org/10.1016/j.optmat.2021.111121.
[2] T. Homann, U. Hotje, M. Binnewies, A. Börger, K.D. Becker, T. Bredow, *Composition-dependent band gap in ZnS_xSe_{1-x}: a combined experimental and theoretical Study,* Solid State Sci. 8, 44 (2006); https://doi.org/10.1016/j.solidstatesciences.2005.08.015.
[3] M. Wang, G.T. Fei, Y.G. Zhang, M.G. Kong, L.D. Zhang, *Tunable and predetermined bandgap emissions in alloyed ZnS_xSe_{1-x} nanowires*, Adv. Mater. 19, 4491 (2007); https://doi.org/10.1002/adma.200602919.
[4] H.X. Chuo, T.Y. Wang, W.G. Zhang, *Optical properties of ZnS_xSe_{1-x} alloy nanostructures and their photodetectors,* J. Alloys Compd. 606, 231 (2014); https://doi.org/10.1016/j.jallcom.2014.04.004.
[5] D. Wu, Y. Chang, Z. Lou, T. Xu, J. Xu, Z. Shi, Y. Tian, X. Li, *Controllable synthesis of ternary ZnS_xSe_{1-x} nanowires with tunable band-gaps for optoelectronic applications*, J. Alloys Compd. 708, 623 (2017); https://doi.org/10.1016/j.jallcom.2017.03.012.
[6] O.P. Malyk, S.V. Syrotyuk, *Heavy hole scattering on intrinsic acceptor defects in cadmium telluride: calculation from the first principles,* Phys. Chem. Solid State, 23(1), 89 (2022); https://doi.org/10.15330/pcss.23.1.89-95.
[7] H.A. Ilchuk, L.I. Nykyruy, A.I. Kashuba, I.V. Semkiv, M.V. Solovyov, B.P. Naidych, V.M. Kordan, L.R. Deva, M.S. Karkulovska, R.Y. Petrus, *Electron, phonon, optical and thermodynamic properties of CdTe crystal calculated by DFT,* Phys. Chem. Solid State, 23(2), 261 (2022); https://doi.org/10.15330/pcss.23.2.261-269.
[8] A.I. Kashuba, B. Andriyevsky, I.V. Semkiv, H.A. Ilchuk, R.Y. Petrus, Ya.M. Storozhuk, *First-principle calculations of band energy structure of $CdSe_{0.5}S_{0.5}$ solid state solution thin films,* Phys. Chem. Solid State, 23, 52 (2022); https://doi.org/10.15330/pcss.23.1.52-56.
[9] Yu-J. Zhao, P. Mahadevan, A. Zunger, *Practical rules for orbital-controlled ferromagnetism of 3d impurities in semiconductors,* J. Appl. Phys.98, 113901 (2005); https://doi.org/10.1063/1.2128470.
[10] Y. Wei, Ch. Liu, E. Ma, T. Wang, W. Jie, *Optical properties of mid-infrared Cr2+:ZnSe single crystals grown by chemical vapor transporting with NH_4Cl*, Opt. Optical Materials Express, 11, 664 (2021); https://doi.org/10.1364/OME.416315.

[11] Y. C. Wei, C. Y. Liu, E. Ma, Z. Y. Lu, F. Y. Wang, Y. C. Song, Q. H. Sun, W. Q. Jie, T. Wang, *The optical spectra characteristic of Cr^{2+}:ZnSe polycrystalline synthesized by direction of Zn-Cr alloy and element Se,* Ceram. Int. 46, 21136 (2020); https://doi.org/10.1016/j.ceramint.2020.05.190.
[12] S.V. Syrotyuk, O.P. Malyk, *Effect of Strong Correlations on the Spin-polarized Electronic Energy Bands of the CdMnTe Solid Solution,* J. Nano- Electron. Phys., 11, 01009 (2019); https://doi.org/10.21272/jnep.11(1).01009).
[13] S.V. Syrotyuk, Moaid K. Hussain, *The Effect of Cr Impurity and Zn Vacancy on Electronic and Magnetic Properties of ZnSe Crystal*, Phys. Chem. Solid State: 22, 529 (2021).
[14] S.V. Syrotyuk, M.K. Hussain, *Influence of Pressure on the Electronic and Magnetic Properties of the ZnSeTe Solid Solution Doped with Fe Atoms*, J. Nano- Electron. Phys., 15, 05002 (2023); https://doi.org/10.21272/jnep.15(5).05002.
[15] S.V. Syrotyuk, A.Y. Nakonechnyi, Yu.V. Klysko, H.I. Vlakh-Vyhrynovska, Z.E. Veres, *Electronic and magnetic properties of ZnSeS solid solution modified by Mn impurity, Zn vacancy and pressure*, Phys. Chem. Solid State, 25, 65 (2024); https://doi.org/10.15330/pcss.25.1.65-72.
[16] [S.V. Syrotyuk, A.Y. Nakonechnyi, Yu.V. Klysko, M.V. Stepanyak, V.M. Myshchyshyn, *Electronic and Magnetic Properties of the Wurtzite Solid Solution Mn:ZnSeS,* J. Nano- Electron. Phys., 16, 05033 (2024); https://doi.org/10.21272/jnep.16(5).05033.
[17] X. Gonze et al., *Recent developments in the ABINIT software package,* Comput. Phys. Comm. 205, 106 (2016); https://doi.org/10.1016/j.cpc.2016.04.003.
[18] P.E. Blöchl, *Projector augmented-wave method*, Phys. Rev. B 50, 17953 (1994); https://doi.org/10.1103/PhysRevB.50.17953.
[19] J.P. Perdew, K. Burke, M. Ernzerhof, *Generalized Gradient Approximation Made Simple*, Phys. Rev. Letters 77, 3865 (1996); https://doi.org/10.1103/PhysRevLett.77.3865.
[20] M. Ernzerhof, G.E. Scuseria, *Assessment of the Perdew–Burke–Ernzerhof exchange-orrelation functional*, J. Chem. Phys. 110, 5029 (1999); https://doi.org/10.1063/1.478401.

С.В. Сиротюк[1], М.К. Хуссейн[2], Р.А. Наконечний[1]

Електронні й магнітні властивості гексагональних твердих розчинів ZnSeS, зумовлені домішкою Cr та концентрацією аніонів

[1]Національний Університет "Львівська політехніка", Львів, Україна, stepan.v.syrotiuk@lpnu.ua;
[2]Кафедра електротехнічної інженерії, Університетський коледж Аль-Хусейна, Кербела, Ірак

Спін-поляризовані електронні енергетичні спектри твердого розчину ZnSeS отримано на основі розрахунків для суперкомірки, що містить 64 атоми. Розраховано електронні властивості матеріалів на основі двох суперелементів, а саме $Zn_{31}Cr_1Se_8S_{24}$ та $Zn_{31}Cr_1Se_{24}S_8$, де Cr заміщує атом Zn. Результати розрахунків показують, що обидва матеріали є напівпровідниками для електронних станів зі спіном вниз. Для протилежного спінового моменту електронів обидва матеріали виявляють металеві стани. Для обох матеріалів встановлено значний вплив домішки заміщення Cr на їхні електронні та магнітні властивості. Обидва досліджені тут матеріали є напівметалами, тому вони є перспективними матеріалами для спінової електроніки.

Ключові слова: Тверді розчини ZnSeS, 3d Домішки, Електронна енергетична структура, Магнітний момент.